Neuroscience
Physics of Living Systems

Detection of changes in membrane potential by magnetic resonance imaging

Reviewed Preprint
v1 • October 28, 2024
Not revised

Kyeongseon Min, Sungkwon Chung, Seung-Kyun Lee, Jongho Lee, Phan Tan Toi, Daehong Kim, Jung Seung Lee, Jang-Yeon Park

Department of Electrical and Computer Engineering, Seoul National University, Seoul, Republic of Korea • Department of Physiology, Sungkyunkwan University School of Medicine, Suwon, Republic of Korea • Department of Biomedical Engineering, Sungkyunkwan University, Suwon, Republic of Korea • Department of Intelligent Precision Healthcare Convergence, Sungkyunkwan University, Suwon, Republic of Korea • National Cancer Center, Goyang, Republic of Korea

eLife Assessment

The authors show MRI relaxation time changes that are claimed to originate from cell membrane potential changes. This would be very **important** if true because it may provide a mechanism whereby membrane potential changes could be inferred noninvasively. However, the membrane potential manipulations applied here will induce cell swelling, and cell swelling has been previously shown to affect relaxation time. Therefore, the claim that the relaxation time changes observed in this manuscript are due to cell membrane potential changes is **inadequately** supported.

https://doi.org/10.7554/eLife.101642.1.sa3

Abstract

Membrane potential plays a crucial role in various cellular functions. However, existing techniques for measuring membrane potential are often invasive or have limited recording depth. In contrast, magnetic resonance imaging (MRI) offers noninvasive imaging with desirable spatial resolution over large areas. This study investigates the feasibility of utilizing MRI to detect membrane potential changes by measuring magnetic resonance parameters while manipulating membrane potential in cultured cells and *in vivo* rat models. Our findings reveal that depolarization (or hyperpolarization) of the membrane potential increases (or decreases) the T_2 relaxation time, while the ratio of bound to free water proton shows the opposite trend. These findings also suggest a pioneering approach to noninvasively detect changes in membrane potential using MRI.

Highlights

- Changes in membrane potential can be detected using magnetic resonance imaging (MRI).
- T_2 relaxation time and magnetization transfer are sensitive to changes in membrane potential.

Introduction

Membrane potential is a fundamental property of all living cells, influencing crucial cell functions[1] such as neuronal and myocyte excitability, volume control, cell proliferation, and secretion. In the fields of neuroscience, membrane potential is of significant importance, as neural activities arise from the dynamic propagation of this electric potential. From a clinical perspective, deviations from normal membrane potential levels contribute to various diseases, including seizures[2], arrhythmia[3], and hypoglycemia[4]. Given its scientific and clinical importance, effective methods to detect changes in membrane potential have long been sought.

The intracellular recording technique using sharp glass electrodes is a commonly used method to detect changes in membrane potential[5,6]. It provides real-time absolute recordings of membrane potential. Optical imaging is another major approach to detect changes in membrane potential. Voltage-sensitive dyes enable voltage imaging at the cellular level[7]. Fluorescent calcium indicators detect calcium transients associated with neuronal activation[8]. Label-free optical imaging techniques[9] utilize various contrast mechanisms such as cell membrane deformation, which are directly coupled with changes in membrane potential. Despite their efficacy, these methods have limitations when applied to intact biological systems due to their invasive nature, requiring procedures such as craniotomy.

As noninvasive techniques for directly or indirectly detecting brain activation *in vivo*, several imaging modalities have been developed, including electroencephalography (EEG)[10], magnetoencephalography (MEG)[11], and magnetic resonance imaging (MRI)[12]. EEG and MEG detect electric potentials on the scalp and extracranial magnetic fields, respectively, which are directly induced by neuronal activity in the brain. Although these techniques are noninvasive and provide excellent temporal resolution of milliseconds or less, they are constrained by shallow imaging depth and spatial localization challenges[13].

In contrast, MRI enables noninvasive imaging with good spatial resolution of millimeters over a large brain volume, making it an appropriate tool for *in vivo* functional brain imaging. To date, the mainstream of functional MRI (fMRI) utilizes hemodynamic responses driven by brain activation, such as the blood oxygen level-dependent (BOLD) effect[14]. However, while the BOLD contrast mechanism reflects dynamic changes in neuronal activity through neurovascular coupling, it provides inherently indirect and relatively slow, hemodynamic-responsive information of brain function[15]. On the other hand, many studies have attempted to explore the possibility of using MRI to directly detect neuronal activity[16,17]. These studies utilized neuronal current-dependent signal phase shifts[18-20] and magnitude decay[21-24], the Lorentz effect[25], high temporal resolution[26,27], ghost artifacts[28], or cell swelling[29,30], while concerns about sensitivity exist[31-36].

In this study, we investigated the possibility of using MRI to detect changes in membrane potential. We explored the dependence of T_2 relaxation time and magnetization transfer (MT) on membrane potential changes, both *in vitro* and *in vivo*. *In vitro* experiments utilized two homogeneous and electrically non-active cells, i.e., neuroblastoma (SH-SY5Y) and leukemia (Jurkat) cell lines, providing a controlled environment free from hemodynamic effects. This aided in accurately evaluating changes in MR parameters with membrane potential. *In vivo* experiments, conducted on a rat model with a craniotomy-exposed cortex, aimed to reproduce the *in vitro* findings.

Results

In vitro changes in MR parameters induced by membrane potential

A non-excitable neuroblastoma cell line, SH-SY5Y, was selected to investigate the relationship between MR parameters and membrane potential. After culturing SH-SY5Y cells, they were suspended in extracellular media with various potassium ion concentrations ($[K^+]$). As the control condition, $[K^+]$ = 4.2 mM was selected. For depolarization conditions, $[K^+]$ = 20, 40, and 80 mM were used. For hyperpolarization conditions, $[K^+]$ = 0.2 and 1 mM were used. The suspended cells were concentrated with centrifugation in an acrylic container and scanned in a 9.4 T preclinical MRI system to measure T_2 and MT parameters such as pool size ratio (PSR) and magnetization transfer rate (k_{mf}) under each condition (**Fig. 1**). The PSR value represents the ratio of hydrogen protons in macromolecules and free water, and k_{mf} represents the magnetization transfer rate of hydrogen protons from macromolecules to free water. In addition, the membrane potential of SH-SY5Y cells in each condition was separately measured via patch clamp recording.

The changes of T_2, PSR, and k_{mf} in SH-SY5Y cells when the membrane potential (V_m) was modulated by varying $[K^+]$ are shown in **Figure 2**, alongside the actual V_m measured via patch clamp recordings. We conducted statistical analyses to assess the effect of changes in V_m from the control condition (ΔV_m) on the MR parameters. A linear mixed-effect model was applied to account for inter-sample variability and repeated measurements. This model included MR parameters as dependent variables, ΔV_m as a fixed effect, and cell batch as a random effect. The analysis yielded the following relationships:

$$T_2\,(\text{ms}) = 49.7\,(1 + 0.00687\,\Delta V_m) \quad \cdots\cdots [1]$$

$$\text{PSR} = 0.0377\,(1 - 0.00542\,\Delta V_m) \quad \cdots\cdots [2]$$

$$k_{mf}\,(\text{Hz}) = 14.8\,(1 + 0.000648\,\Delta V_m) \quad \cdots\cdots [3]$$

The effects of ΔV_m on T_2 and PSR were both significant ($p < 0.0001$), indicating an increase in T_2 and a decrease in PSR during depolarization, with the opposite trend during hyperpolarization. On the other hand, the effect of ΔV_m on k_{mf} was not significant ($p = 0.360$).

Subsequent post-hoc analyses compared each experimental condition to the control using Dunnett's test to account for multiple comparisons (**Fig. 2**). During depolarization induced by the highest $[K^+]$ (80 mM, ΔV_m = 30.0 mV), changes in MR parameters were observed as a 20.0% increase in T_2 (ΔT_2 = 10.1 ms, $p < 0.0001$) and a 12.9% decrease in PSR (ΔPSR = −0.00476, $p < 0.0001$). Conversely, during hyperpolarization induced by the lowest $[K^+]$ (0.2 mM, ΔV_m = −5.33 mV), T_2 decreased by 4.40% (ΔT_2 = −2.21 ms, $p < 0.0001$) and PSR increased by 6.28% (ΔPSR = 0.00231, $p < 0.0005$). However, changes in k_{mf} were not significant across all conditions ($p > 0.05$). These findings from *in vitro* SH-SY5Y cell experiments suggest that MR parameters, such as T_2 and PSR, exhibit sufficient sensitivity to detect alterations in membrane potential, both depolarization and hyperpolarization.

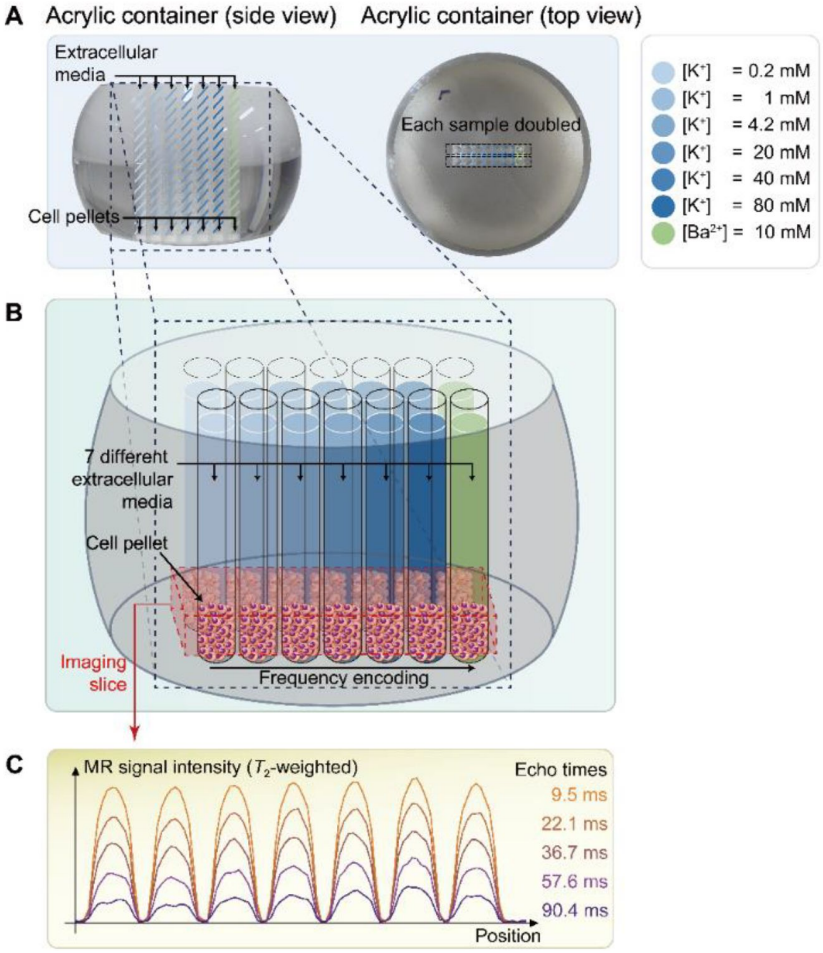

Fig. 1.

The schematic diagram of the *in vitro* experiment. (A) The picture on the left displays a side view of a double-sided cut spherical acrylic container with fabricated wells filled with extracellular media and cell pellets. As depicted in the top-view picture on the right, fourteen wells (matrix = 2 × 7) were created on the acrylic container, allowing each of the seven samples with six different K^+ concentrations ($[K^+]$ = 0.2–80 mM) and one Ba^{2+} concentration ($[Ba^{2+}]$ = 10 mM) to be doubled in the same column for improved signal-to-noise ratio (SNR) in MR signal acquisition. (B) The image illustrates the configuration after loading cells into the wells and pelleting them at the bottom of the wells. (C) Representative one-dimensional T_2-weighted MR signals with different echo times.

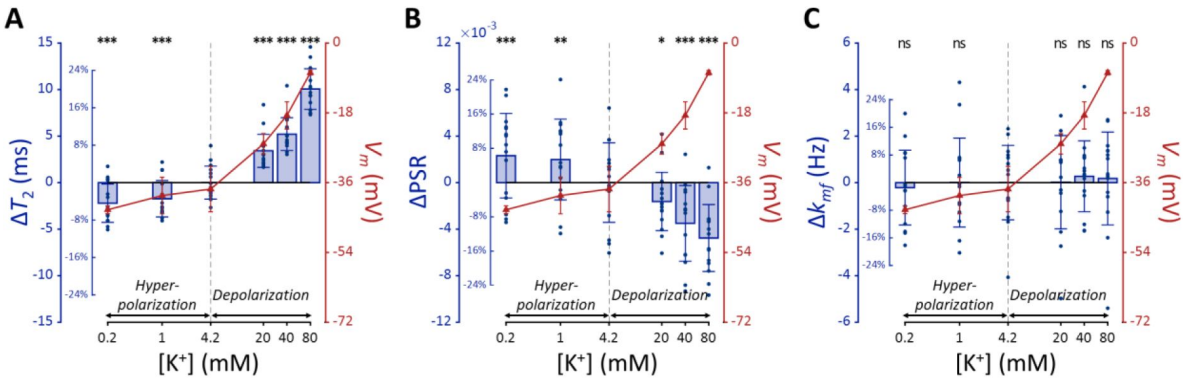

Fig. 2.

MR parameters and membrane potential (V_m) of SH-SY5Y cells versus extracellular K^+ concentrations ([K^+]). Changes in (A) T_2, (B) PSR, and (C) k_{mf} are displayed with blue bars (n = 15). Membrane potentials are plotted with red triangles (n = 3). The abscissa is in logarithmic scale. Error bars denote standard deviation. Statistical significance of changes in MR parameters is marked with asterisks (ns: $p > 0.05$, *: $p < 0.05$, **: $p < 0.01$, ***: $p < 0.001$).

Using a K^+ channel blocker

In this experiment, we investigated whether depolarization induced by altering potassium permeability with barium ions (Ba^{2+}) would affect MR parameters similarly to depolarization induced by varying [K^+], thereby further validating our findings. For this purpose, we administered barium ions (Ba^{2+}) at a concentration of 10 mM to induce depolarization. Ba^{2+} was chosen because it inhibits several types of two-pore-domain potassium channels[37,38], which predominantly regulate the resting membrane potential. Previous studies have confirmed that Ba^{2+} depolarizes the membrane potential in SH-SY5Y and Jurkat cells[39,40].

The Ba^{2+}-induced depolarization condition was compared with K^+-induced depolarization and hyperpolarization conditions (**Fig. 3**). To compare the effects of [Ba^{2+}] and [K^+] on MR parameters, a linear mixed-effect model was utilized. This model included MR parameters as dependent variables, ΔV_m and its interaction with a group variable (indicating whether ΔV_m was induced by [Ba^{2+}] or [K^+]) as fixed effects, and cell batch as a random effect. This analysis revealed no significant interactions for all MR parameters assessed (p = 0.182 for T_2, p = 0.788 for PSR, and p = 0.0890 for k_{mf}). These findings suggest that changes in T_2 and PSR by membrane potential do not depend on the specific method of altering the membrane potential, whether by varying [K^+] or applying [Ba^{2+}]. This implies that if the changes in MR parameters observed with varying [K^+] were not primarily due to membrane potential but were due to other K^+-related factors, then experiments using [Ba^{2+}] would not result in similar changes.

Subsequent post-hoc analyses compared the [Ba^{2+}]-induced depolarization to the control using Dunnett's test to account for multiple comparisons (**Fig. 3**). In response to depolarization caused by [Ba^{2+}] = 10 mM, T_2 increased by 7.82% (ΔT_2 = 3.93 ms, p < 0.0001) and PSR decreased by 8.06% (ΔPSR = −0.00297, p < 0.0001). The change in k_{mf} was not significant (Δk_{mf} = −0.832 Hz, p = 0.263). The depolarization of membrane potential induced by [Ba^{2+}] was measured as ΔV_m = 13.3 mV by patch clamp recording.

Using another cell type

To investigate whether changes in MR parameters in response to membrane potential differ across cell types, we assessed another cell line, Jurkat, under the same experimental conditions applied to SH-SY5Y cells. These conditions included a control condition at [K^+] = 4.2 mM; hyperpolarization conditions at [K^+] = 0.2 and 1 mM; depolarization conditions at [K^+] = 20, 40, and 80 mM; and a Ba^{2+}-induced depolarization condition at 10 mM.

Each experimental condition was compared to the control using Dunnett's test to account for multiple comparisons (**Fig. 4**). As observed with SH-SY5Y cells, Jurkat cells showed significant positive changes in T_2 and negative changes in PSR during depolarization. For example, at [K^+] = 80 mM, T_2 increased by 16.9% (ΔT_2 = 9.26 ms, p < 0.0001), PSR decreased by 21.9% (ΔPSR = −0.00347, p < 0.01). In contrast, during hyperpolarization at the lowest [K^+] = 0.2 mM, T_2 decreased by 18.1% (ΔT_2 = −9.93 ms, p < 0.0001), whereas PSR increased by 17.6% (ΔPSR = 0.00280, p < 0.05). The depolarization induced by [Ba^{2+}] = 10 mM resulted in a similar pattern, with T_2 increasing by 11.5% (ΔT_2 = 6.3 ms, p < 0.0005), although the decrease in PSR was not significant (ΔPSR = −0.00212, p = 0.211). Changes in k_{mf} remained non-significant across all conditions (p > 0.05). In summary, these findings indicate that the detectability of membrane potential changes by MR parameters like T_2 and PSR does not appear specific to cell type, although the magnitude of these changes varies between different cell types.

Fig. 3.

Changes in (A) T_2, (B) PSR, and (C) k_{mf} of SH-SY5Y cells across experimental conditions: $[K^+]$ = 0.2–80 mM (blue cross) and $[Ba^{2+}]$ = 10 mM (green triangle), compared to the control condition (black cross). Data from fifteen experiments (n = 15) are displayed. Linear regression lines for $[K^+]$ data (blue solid line) and $[Ba^{2+}]$ data (green solid line) are drawn along with dotted lines representing 95% confidence intervals. Error bars denote standard deviation. Statistical significance of changes in MR parameters with $[Ba^{2+}]$ = 10 mM is marked with asterisks (ns: $p > 0.05$, *: $p < 0.05$, **: $p < 0.01$, ***: $p < 0.001$).

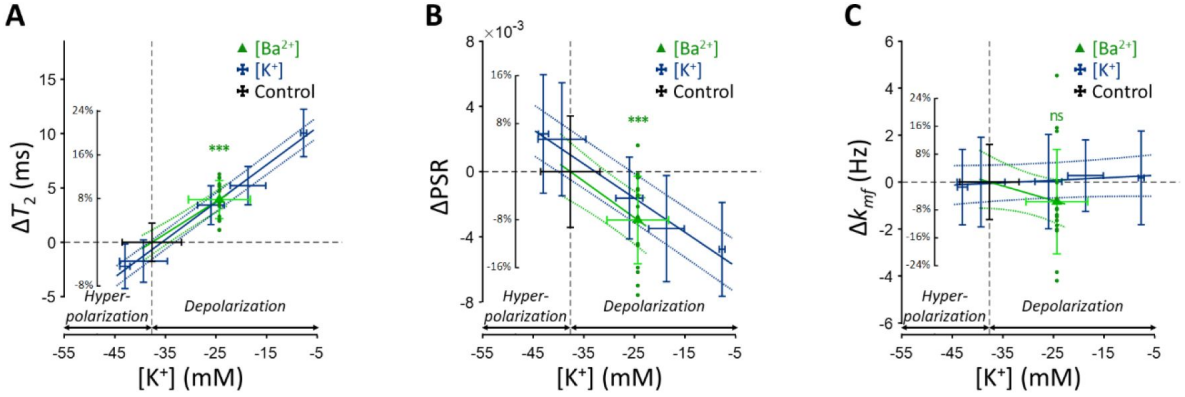

Fig. 4.

Changes in (A) T_2, (B) PSR, and (C) k_{mf} of Jurkat cells across experimental conditions: $[K^+]$ = 0.2–80 mM (blue bar) and $[Ba^{2+}]$ = 10 mM (green bar), compared to the control condition of $[K^+]$ = 4.2 mM (n = 5). Error bars denote standard deviation. Statistical significance of changes in MR parameters is marked with asterisks (ns: $p > 0.05$, *: $p < 0.05$, **: $p < 0.01$, ***: $p < 0.001$).

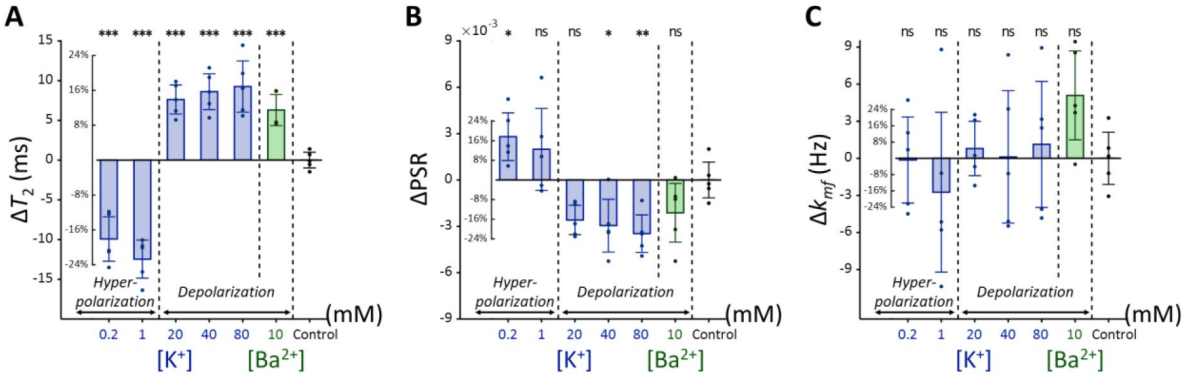

In vivo changes in T_2 by membrane potential

The dependence of T_2 values on membrane potential, observed in the aforementioned SH-SY5Y and Jurkat cell studies, was further explored in an *in vivo* rat model to validate these findings under physiological conditions. As depicted in **Figure 5**, a craniotomy was performed to expose a 3-mm-diameter region of the rat cerebral cortex, followed by perfusion with artificial cerebrospinal fluid (aCSF) to modulate the membrane potential. Hemodynamic responses were pharmacologically suppressed. MRI scans were performed using a 7 T preclinical MRI system to measure T_2 in the exposed cortical area. A total of seven rats were used in the experiment that involved modulation of $[K^+]$. The experimental protocol included sequential application of four conditions, each lasting 12 minutes: a baseline condition at $[K^+]$ = 3 mM, a depolarization condition at $[K^+]$ = 40 mM, further depolarization at $[K^+]$ = 80 mM, followed by a recovery condition using baseline aCSF. The recovery condition was applied to two of the seven rats. To distinguish the effect of aCSF perfusion on T_2 from the effect of changes in membrane potential, a control experiment was also conducted using only baseline aCSF for the entire duration (48 minutes) with another group of five rats.

In **Figure 6A**, a representative T_2 map is displayed with an enlarged image defining the ROI beneath the perfusion chamber (width = 1.8 mm, depth = 0.6mm). The average T_2 value within this ROI was estimated from the spatially averaged multi-echo spin-echo signal. A detailed analysis on the quality of these T_2 maps is presented in Supplementary Results S2.1. Changes in T_2 value (ΔT_2) were statistically analyzed using a linear mixed-effect model to account for inter-sample variability and repeated measurements. This model included ΔT_2 as a dependent variable, elapsed time and its interaction with the experiment type (i.e., $[K^+]$-modulation or control) as fixed effects, and a random effect for inter-sample variability.

Figure 6B shows the results of the statistical analysis. ΔT_2 values were plotted against elapsed time for $[K^+]$-modulation and control experiments. After 12 minutes from the initial condition, T_2 increased by 1.46% (ΔT_2 = 0.684 ms) in the $[K^+]$-modulation experiment ($[K^+]$ = 40 mM) and by 0.223% (ΔT_2 = 0.104 ms) in the control experiment ($[K^+]$ = 3 mM); the ΔT_2 difference (= 0.580 ms) between these experiments was not statistically significant (p = 0.0711). After 24 minutes, T_2 increased by 2.34% (ΔT_2 = 1.10 ms) in the $[K^+]$-modulation experiment ($[K^+]$ = 80 mM) and by 0.386% (ΔT_2 = 0.181 ms) in the control experiment ($[K^+]$ = 3 mM), with a significant difference in ΔT_2 (= 0.918 ms) between them (p = 0.00172). Due to the limited sample size in the recovery phase (n = 2 out of 7 for $[K^+]$-modulation), comparisons between experiments were not conducted for this recovery phase.

Our observations indicate that *in vivo* manipulation of membrane potential results in similar trends of T_2 changes as those observed *in vitro*, albeit with a smaller magnitude in the rat cortex. This discrepancy may be attributed to several factors: $[K^+]$-modulation affecting only a small portion of cells within the ROI; limited diffusion of aCSF through the leptomeninges; removal of excessive K^+ through clearing mechanisms; and differences in cell types (see the Discussion for more details).

Discussion

In this study, we demonstrated that MR parameters, specifically T_2 relaxation time and pool size ratio (PSR), can detect changes in membrane potential. To the authors' knowledge, this is the first report that changes in membrane potential can be detected through MRI, which has the advantage of noninvasively acquiring signals over a large area with good spatial resolution. Our *in vitro* experiments with cultured cells were designed to exclude physiological factors such as

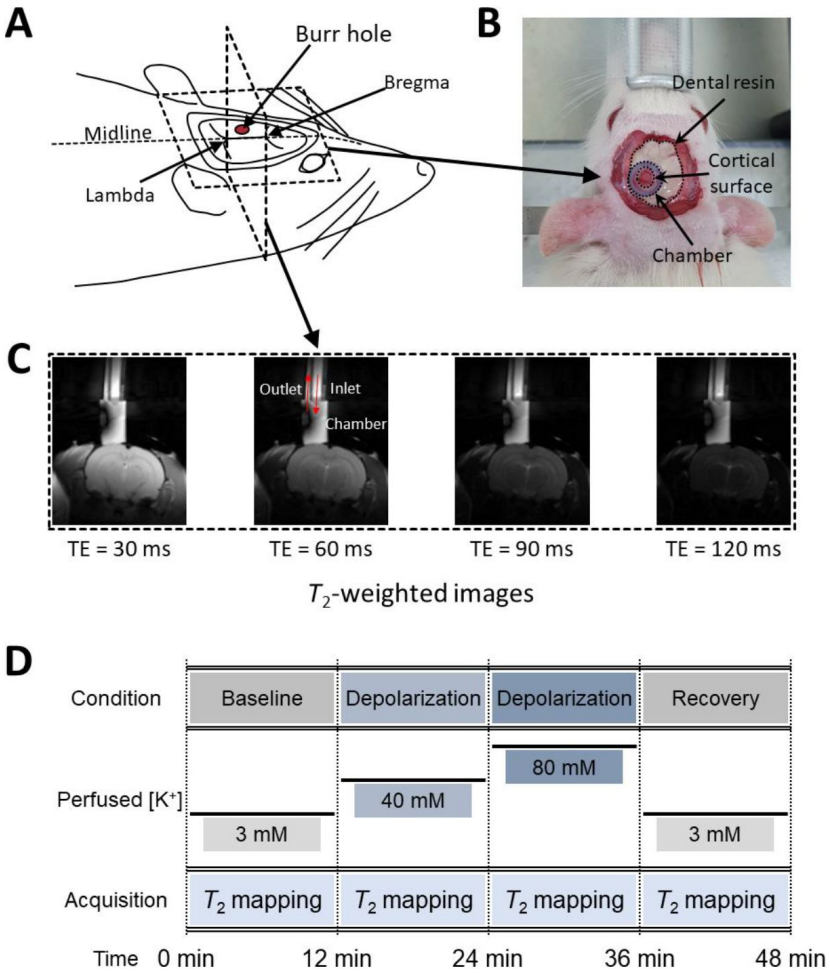

Fig. 5.

Experimental setup for *in vivo* manipulation of membrane potential. (A) A schematic diagram of the rat head post-craniotomy, showing the burr hole centered at 2.5 mm anterior and 2.0 mm lateral to the lambda. (B) Photograph of the rat head with a cylindrical chamber fixed over the burr hole, filled with artificial cerebrospinal fluid. (C) A representative series of T_2-weighted MR images for T_2 mapping. The chamber was connected to inlet and outlet perfusion tubes. (D) The experimental paradigm of the *in vivo* rat MR imaging. Four conditions were sequentially applied: control, depolarization, further depolarization, and recovery. Each condition lasted 12 minutes during which T_2 mapping were conducted.

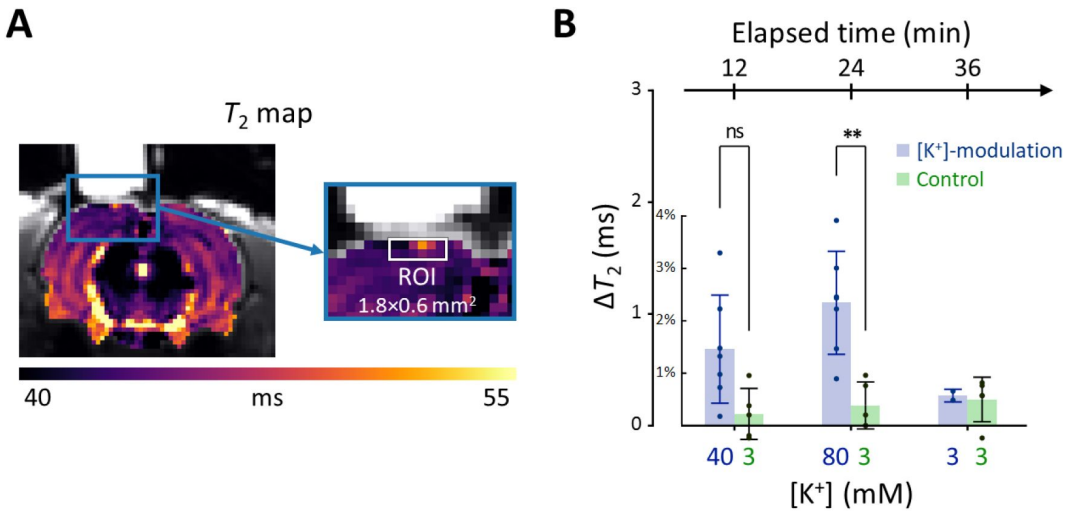

Fig. 6.

Results of the *in vivo* experiment results in rat models. (A) A representative T_2 map from a single rat with an enlarged image depicting the ROI for estimating average T_2 in the exposed cortical area, marked by a white rectangle (width = 1.8 mm, depth = 0.6 mm). (B) The changes in T_2 values within the ROI is plotted against elapsed time from the initial conditions. $[K^+]$ in the perfused artificial cerebrospinal fluid are indicated on the bottom abscissa. Results from the $[K^+]$-modulation experiments are shown with blue bars, and those from the control experiments are shown with green bars. Statistical significance of the T_2 changes are marked with asterisks (ns: $p > 0.05$, *: $p < 0.05$, **: $p < 0.01$).

hemodynamic responses and respiration. We observed that depolarization increases T_2 and decreases PSR, while hyperpolarization has the opposite effect. *In vivo*, we pharmacologically suppressed hemodynamic responses to minimize their impact on T_2 measurements. The trend of T_2 dependence on membrane potential *in vivo* was consistent with *in vitro* findings. However, the magnitude of T_2 changes in rat cortex was approximately one-ninth of that observed in SH-SY5Y cells *in vitro* at $[K^+]$ = 80 mM.

Several factors may contribute to discrepancies between *in vivo* and *in vitro* results. For instance, the actual extracellular $[K^+]$ experienced by cells in the rat cortex may be lower than that of the perfused aCSF due to diffusion-limiting barriers such as the leptomeninges[41,42], even after the removal of the dura mater. Additionally, removal of excessive K^+ by clearing mechanisms[43,44] may further reduce the $[K^+]$ experienced by the cells. Partial volume effects and cell type differences may also contribute to the discrepancy.

From a biophysical perspective, changes in T_2 and PSR due to changes in membrane potential may be attributed to changes in cell volume, hydration water, and bulk water. These factors have also been suggested as potential mechanisms underlying diffusion fMRI[29,45,46]. Here, hydration water is known to have a significantly shorter T_2 than bulk water[47], and depolarization or hyperpolarization is known to be accompanied by cell swelling or shrinking, respectively[48-50]. To be more specific, according to the definition of PSR as the ratio of bound to free water protons, the observed decrease in PSR upon depolarization indicates that the amount of bulk water with much longer T_2 becomes relatively greater in the voxel than hydration water with much shorter T_2, which can lead to an overall increase in T_2. It could be hypothesized that T_1 would behave similarly to T_2 under membrane potential changes. For reference, we also conducted T_1 measurements (Supplementary Fig. S2–4), demonstrating that T_1 trends in a manner similar to T_2 in response to membrane potential changes, while it is 3.5 times less sensitive than T_2.

Several challenges and considerations were addressed in this study. First, maintaining the desired environment (37°C and 5% CO_2) for *in vitro* cells during MRI scans is challenging. In addition, intracellular accumulation of Ba^{2+} in the Ba^{2+}-induced depolarization experiment may affect cellular integrity. In this study, high cell viability (> 97.6%) was confirmed using cell viability assays under experimental conditions (Supplementary Fig. S5). Second, differences in T_2 value among the extracellular media may bias T_2 measurements due to the partial volume effect. However, in this study, the differences in T_2 among the extracellular media were found to be negligible compared to the observed T_2 changes (Supplementary Fig. S6). Third, while our findings show that changes in membrane potential can affect MR parameters, it is important to note that these changes do not measure the membrane potential itself. Fourth, other factors such as pH, energy depletion, or extracellular osmolarity may affect MR parameters by altering cell volume. To minimize the effects of these other contributors, we matched osmolarity across all conditions, provided sufficient glucose to prevent energy depletion, and regulated pH levels by buffering with HEPES. Additionally, to mitigate possible changes in intra/extracellular volume fraction changes caused by cell movements, potentially due to agitation, we centrifuged the cells and imaged the bottom portion of the cell pellet, where cell movement was restricted due to close packing. Finally, our experimental paradigm was based on clamping the membrane potential at a specific level, thus measuring changes in T_2 and PSR during static depolarization or hyperpolarization rather than dynamic changes such as those seen during action potentials. Future research could explore temporally varying membrane potential to evaluate the dynamic correlation between membrane potential and MR parameters with high temporal resolution MRI[26,27].

In summary, our study demonstrates that MR parameters such as T_2 relaxation time can reflect changes in membrane potential both *in vitro* and *in vivo*. This finding proposes a pioneering approach for noninvasively detecting changes in membrane potential using MRI.

Methods

In vitro cell culture

Two human cell lines were utilized for the experiments: SH-SY5Y, an immortalized neuroblastoma line, and Jurkat, a leukemia cell line. Both cell lines were sourced from the American Type Culture Collection (ATCC). The SH-SY5Y cells were cultured in DMEM/F12 medium supplemented with 10% (v/v) fetal bovine serum (FBS) and 100 U/ml penicillin/streptomycin. The cells were maintained at a constant temperature of 37°C in a humidified atmosphere containing 5% CO_2. Similarly, the Jurkat cells were cultured in RPMI-1640 medium, also supplemented with 10% (v/v) FBS and 100 U/ml penicillin/streptomycin, under the same conditions of temperature and CO_2 concentration.

In vitro manipulation of membrane potential with extracellular media

The baseline extracellular medium was prepared with the following components: KCl = 4.2 mM; NaCl = 145.8 mM; HEPES = 20 mM; glucose = 4.5 g/l; EGTA = 10 μM; pH = 7.2. This baseline medium was considered a control condition for various extracellular media used to adjust membrane potential. Two extracellular media with low K^+ concentrations (KCl = 0.2 and 1 mM) were prepared to hyperpolarize the membrane potential. Three extracellular media with high K^+ concentrations (KCl = 20, 40, and 80 mM) were prepared to depolarize the membrane potential. A Ba^{2+} medium containing 10 mM $BaCl_2$ was also prepared to depolarize the membrane potential in a different way, i.e., as a K^+ channel blocker. These seven extracellular media were used for both MR imaging and patch clamp recording *in vitro*. Sodium ion concentrations ($[Na^+]$) in all media were controlled to match the osmolarity with the baseline medium. The composition of all extracellular media is detailed in Supplementary Table S3.

Preparation of cells for *in vitro* MR measurement

SH-SY5Y cells were harvested and concentrated into a pellet (~70 μl) by centrifugation at 250 × g for two minutes. The pellet was resuspended in the culture medium and divided evenly into seven aliquots. Each cell suspension was centrifuged and resuspended in each of the seven different media specified in Supplementary Table S3. Centrifugation and resuspension were repeated three more times to completely clear out the culture medium. Each cell suspension with a different extracellular medium was then loaded into two wells on the same column of an acrylic container with 14 wells (matrix = 2 × 7) and centrifuged again to concentrate into pellets (**Fig. 1**). The acrylic container was purposely formed into a spherical segment to enhance the homogeneity of the static magnetic field[51]. The preparation of Jurkat cell samples was the same as for the SH-SY5Y cell samples.

In vitro MRI experiment

In vitro MRI experiments were performed on a 9.4 T MRI system (BioSpec 94/30 USR, Bruker BioSpin) at room temperature. A volume coil with an inner diameter of 86 mm was utilized for both radiofrequency (RF) pulse transmission and signal reception. Within the acrylic container, two wells on the same column (matrix = 2 × 7) contained identical cell pellets with the same extracellular media. MRI signals from seven different cell samples in the horizontal direction were separated by one-dimensional frequency encoding along that direction (**Fig. 1**). The MRI pulse sequence employed for mapping the T_2 value was a single-echo spin-echo (SESE) sequence with 50 variable echo times (TE) spaced between 9.5 and 290.5 ms on a logarithmic scale. For mapping the MT parameters, an inversion recovery multi-echo spin-echo (IR-MESE) sequence was used. The inversion times (TI) for the IR-MESE sequence were optimized using the theory of Cramér-Rao lower bounds[52]. The optimized TIs ranged from 4 to 10,079.4 ms. After each TI, 16 spin-echo

trains were acquired with an echo spacing of 9.5 ms. Total scan time for both sequences was 23 minutes. Experiments were repeated 15 times for SH-SY5Y cells and 7 times for Jurkat cells, replacing cells in each repetition. Other scan parameters are detailed in Supplementary Table S1.

Animals

Male Wistar rats aged 8 weeks (250–300 g, Orient Bio) were used for MRI experiments after undergoing a craniotomy. All animal experiments were approved by the Institutional Animal Care and Use Committee at the National Cancer Center Korea (NCC-22-740). The rats were housed in ventilated cages under a 12h/12h light/dark cycle and provided with *ad libitum* access to food and water.

In vivo manipulation of membrane potential with artificial cerebrospinal fluid (aCSF)

The membrane potential of the exposed cortex was manipulated by directly perfusing the region-of-interest of the cerebral cortex with aCSF after a craniotomy. The baseline aCSF was prepared with the following components: KCl = 3 mM; NaCl = 135 mM; $MgCl_2$ = 3 mM; HEPES = 20 mM; glucose = 4.5 g/l; EGTA = 2 mM; N_ω-Nitro-L-arginine = 1 mM; Nifedipine = 0.1 mM; pH = 7.4. Hemodynamic effects were pharmacologically suppressed using N_ω-Nitro-L-arginine, Nifedipine, and EGTA. N_ω-Nitro-L-arginine suppresses depolarization-induced hemodynamic response by blocking the synthesis of nitric oxide, which acts as a vasodilator[53]. Nifedipine blocks voltage-sensitive Ca^{2+} channels, and EGTA chelates free Ca^{2+} to inhibit the hemodynamic response[54]. To induce depolarization, aCSF with high $[K^+]$ (KCl = 40 and 80 mM) was prepared. The osmolarity of the aCSF was matched with the concentration of NaCl.

Rat surgery

A craniotomy was performed on a Wistar rat. The experimental setup after a surgical procedure is illustrated in **Figure 5**. The surgery was performed following an established protocol[55] alike to that used in other MRI studies[56,57]. Anesthesia was induced with 3% isoflurane in O_2 and maintained with 2–3% isoflurane during the surgical procedure. Body temperature was maintained at 36.5–37.5°C with an infrared lamp. The head was fixed with a small animal stereotaxic frame. The hair on the scalp was shaved with a veterinary clipper. The skin and periosteum over the skull were removed using a scalpel and surgical scissors. A 3.0-mm-diameter burr hole was opened using a dental drill with its center at the coordinates of 2.5 mm anterior and 2.0 mm lateral to the lambda. Then, a cylindrical chamber was implanted upon the burr hole with cyanoacrylate glue and dental composite resin. The chamber was filled with the baseline aCSF and connected to inlet and outlet perfusion tubes. The exposed cerebral cortex inside the chamber was perfused with the baseline aCSF at a flow rate of 0.6 ml/min using peristaltic pumps.

In vivo MRI experiment

The rat with a cranial chamber installed on the cortical surface was placed on a 7 T MRI system (BioSpec 70/20 USR, Bruker BioSpin), fixed in a customized cradle with two ear-bars and a bite-bar. A customized surface coil (rectangular, 35 mm × 20 mm) was used for RF pulse transmission and signal reception. Body temperature was maintained at 36.5–37.5°C using a warm air blower. Anesthesia was maintained with 2% isoflurane in O_2 (0.6 l/min). Respiration rate and body temperature were monitored throughout the MRI experiment. MR images were acquired in a 2 mm coronal slice through the center of the burr hole (**Fig. 5**), using a multi-echo spin-echo (MESE) sequence with 20 TEs (7.5 to 150 ms). Other scan parameters are detailed in Supplementary Table S2.

A total of seven rats were subjected to four sequential experimental conditions, as depicted in **Figure 5**. First, the exposed cerebral cortex was perfused with baseline aCSF ($[K^+]$ = 3 mM). Second, as a depolarizing condition, the perfusion media was switched to depolarizing aCSF of $[K^+]$ = 40 mM. Third, membrane potential was further depolarized by perfusion with aCSF of $[K^+]$ = 80 mM. Finally, as a recovery condition, the perfused aCSF was changed back to baseline aCSF. During each condition, MR images were acquired with MESE sequences for 12 minutes. Two rats underwent the whole four conditions, while other five rats did not undergo the recovery condition. As a control experiment, another set of rats (n = 5) underwent perfusion with the baseline aCSF for the same duration (48 minutes) as the previous experiment, and MR images were acquired with four MESE sequences, each for 12 minutes. Throughout the experiment, the perfusion rate was maintained at 0.6 ml/min.

Quantification of MR parameters

For the *in vivo* MR images acquired with a MESE sequence, echo trains were matched with a simulated dictionary of decay curves of multi-echo spin-echo signals created with the stimulated echo and slice profile correction[58] to estimate T_2 values. For the *in vitro* one-dimensional MR images acquired with the SESE sequence, signals were fitted to a mono-exponential function to estimate T_2 values. For the *in vitro* one-dimensional MR images acquired with the IR-MESE sequence, signals were fitted to a bi-exponential function[59,60] to estimate MT parameters. 16 spin echoes acquired after each TI were averaged to improve SNR. The MT parameters such as PSR and k_{mf} were derived from this fitting process. The detailed procedure for calculating T_2 and two MT parameters (i.e., PSR and k_{mf}) is provided in Supplementary Methods S1.1.

Patch clamp recordings

The membrane potential of SH-SY5Y cells was recorded at room temperature using the whole-cell mode of the patch clamp technique[61]. The bath solution was the same as the extracellular medium used in the MRI experiment and was constantly perfused at a flow rate of 2 ml/min. The composition of the pipette solution was as follows: KCl = 140 mM; NaCl = 5 mM; MgCl2 = 3 mM; HEPES = 10 mM; Mg-ATP = 1 mM; Na-GTP = 0.5 mM. The pH of the pipette solution was adjusted to 7.4 using KOH. Calcium ions (Ca^{2+}) were not included in the pipette solution to minimize Ca^{2+}-dependent currents. The resistance of the electrode was 3–5 MΩ with the internal solution filled. Recordings were performed with a patch amplifier (Axopatch-1D; Axon Instruments) and a current clamp was also used to monitor the membrane potential. The experiment was repeated three times, with cells replaced at each repetition.

Acknowledgements

We thank Dr. Silvia Mangia for insightful discussions on the role of hydration water in functional MRI. Animal molecular imaging facility at the National Cancer Center Korea contributed for supportive animal magnetic resonance imaging. We thank Minsun Kim and Soyeon Jeon (National Cancer Center) for helping with rat craniotomies and MRI experiments. This work was supported by the National Research Foundation of Korea grant funded by the Ministry of Science and ICT (NRF-2019M3C7A1031993, NRF-2019M3C7A1031994, and NRF-2023R1A2C3007075). This work was supported by the Commercialization Promotion Agency for R&D Outcomes (COMPA) funded by the Ministry of Science and ICT (NTIS1711198890).

Additional information

Author contributions

Conceptualization: K.M., S.-K.L., and J.-Y.P. **Methodology**: K.M., S.C., S.-K.L., J.L., P.T.T., D.K., J.S.L., and J.-Y.P. **Investigation**: K.M., S.C., P.T.T., and D.K.; **Resources**: S.C., J.L., D.K., J.S.L., and J.-Y.P. **Visualization**: K.M., and S.C. **Supervision**: J.L., and J.-Y.P. **Writing – original draft** K.M., and J.-Y.P. **Writing – review & editing**: K.M., S.C., S.-K.L., J.L., P.T.T., D.K., J.S.L., and J.-Y.P.

Declaration of interests

The authors declare no competing interests.

Data availability

The data that support the findings of this study are available from the corresponding author upon reasonable request.

References

1. Abdul Kadir L., Stacey M., Barrett-Jolley R. (2018) **Emerging roles of the membrane potential: Action beyond the action potential** *Frontiers in Physiology* **9** https://doi.org/10.3389/fphys.2018.01661

2. Jefferys J.G.R. (1995) **Nonsynaptic modulation of neuronal activity in the brain: Electric currents and extracellular ions** *Physiological Reviews* **75**:689–723 https://doi.org/10.1152/physrev.1995.75.4.689

3. Helfant R.H. (1986) **Hypokalemia and arrhythmias** *The American Journal of Medicine* **80**:13–22 https://doi.org/10.1016/0002-9343(86)90336-0

4. Kane C., Shepherd R.M., Squires P.E., Johnson P.R.V., James R.F.L., Milla P.J., Aynsley-Green A., Lindley K.J., Dunne M.J. (1996) **Loss of functional KATP channels in pancreatic β-cells causes persistent hyperinsulinemic hypoglycemia of infancy** *Nature Medicine* **2**:1344–1347 https://doi.org/10.1038/nm1296-1344

5. Ling G., Gerard R.W. (1949) **The normal membrane potential of frog sartorius fibers** *Journal of Cellular and Comparative Physiology* **34**:383–396 https://doi.org/10.1002/jcp.1030340304

6. Neher E., Sakmann B. (1976) **Single-channel currents recorded from membrane of denervated frog muscle fibres** *Nature* **260**:799–802 https://doi.org/10.1038/260799a0

7. Tasaki I., Watanabe A., Sandlin R., Carnay L. (1968) **Changes in fluorescence, turbidity, and birefringence associated with nerve excitation** *P Natl Acad Sci USA* **61**:883–888 https://doi.org/10.1073/pnas.61.3.883

8. Tsien R.Y. (1980) **New calcium indicators and buffers with high selectivity against magnesium and protons: Design, synthesis, and properties of prototype structures** *Biochemistry-Us* **19**:2396–2404 https://doi.org/10.1021/bi00552a018

9. Zhou Y., Liu E., Müller H., Cui B. (2021) **Optical electrophysiology: Toward the goal of label-free voltage imaging** *J Am Chem Soc* **143**:10482–10499 https://doi.org/10.1021/jacs.1c02960

10. Berger H. (1929) **Über das elektrenkephalogramm des menschen** *Archiv für Psychiatrie und Nervenkrankheiten* **87**:527–570 https://doi.org/10.1007/BF01797193

11. Cohen D. (1968) **Magnetoencephalography: Evidence of magnetic fields produced by alpharhythm currents** *Science* **161**:784–786 https://doi.org/10.1126/science.161.3843.784

12. Mansfield P. (1977) **Multi-planar image formation using NMR spin echoes** *Journal of Physics C: Solid State Physics* **10**:L55–L58 https://doi.org/10.1088/0022-3719/10/3/004

13. He B., Sohrabpour A., Brown E., Liu Z. (2018) **Electrophysiological source imaging: A noninvasive window to brain dynamics** *Annu Rev Biomed Eng* **20**:171–196 https://doi.org/10.1146/annurev-bioeng-062117-120853

14. Ogawa S., Lee T.-M., Nayak A.S., Glynn P. (1990) **Oxygenation-sensitive contrast in magnetic resonance image of rodent brain at high magnetic fields** *Magnetic Resonanace in Medicine* **14**:68–78 https://doi.org/10.1002/mrm.1910140108

15. Logothetis N.K., Pauls J., Augath M., Trinath T., Oeltermann A. (2001) **Neurophysiological investigation of the basis of the fMRI signal** *Nature* **412**:150–157 https://doi.org/10.1038/35084005

16. Bandettini P.A., Petridou N., Bodurka J. (2005) **Direct detection of neuronal activity with MRI: Fantasy, possibility, or reality?** *Applied Magnetic Resonance* **29**:65–88 https://doi.org/10.1007/BF03166956

17. Roth B.J. (2023) **Can MRI be used as a sensor to record neural activity?** *Sensors* **23** https://doi.org/10.3390/s23031337

18. Petridou N., Plenz D., Silva A.C., Loew M., Bodurka J., Bandettini P.A. (2006) **Direct magnetic resonance detection of neuronal electrical activity** *P Natl Acad Sci USA* **103**:16015–16020 https://doi.org/10.1073/pnas.0603219103

19. Wijesinghe R.S., Roth B.J. (2009) **Detection of peripheral nerve and skeletal muscle action currents using magnetic resonance imaging** *Annals of Biomedical Engineering* **37**:2402–2406 https://doi.org/10.1007/s10439-009-9762-6

20. Sundaram P., Nummenmaa A., Wells W., Orbach D., Orringer D., Mulkern R., Okada Y. (2016) **Direct neural current imaging in an intact cerebellum with magnetic resonance imaging** *NeuroImage* **132**:477–490 https://doi.org/10.1016/j.neuroimage.2016.01.059

21. Kamei H., Iramina K., Yoshikawa K., Ueno S. (1999) **Neuronal current distribution imaging using magnetic resonance** *IEEE Transactions on Magnetics* **35**:4109–4111 https://doi.org/10.1109/20.800771

22. Xiong J., Fox P.T., Gao J.-H. (2003) **Directly mapping magnetic field effects of neuronal activity by magnetic resonance imaging** *Human Brain Mapping* **20**:41–49 https://doi.org/10.1002/hbm.10124

23. Chow L.S., Cook G.G., Whitby E., Paley M.N.J. (2006) **Investigating direct detection of axon firing in the adult human optic nerve using MRI** *NeuroImage* **30**:835–846 https://doi.org/10.1016/j.neuroimage.2005.10.024

24. Truong T.-K., Roberts K.C., Woldorff M.G., Song A.W. (2019) **Toward direct MRI of neuro-electro-magnetic oscillations in the human brain** *Magnet Reson Med* **81**:3462–3475 https://doi.org/10.1002/mrm.27654

25. Truong T.-K., Song A.W. (2006) **Finding neuroelectric activity under magnetic-field oscillations (NAMO) with magnetic resonance imaging in vivo** *P Natl Acad Sci USA* **103**:12598–12601 https://doi.org/10.1073/pnas.0605486103

26. Sundaram P., Wells W.M., Mulkern R.V., Bubrick E.J., Bromfield E.B., Münch M., Orbach D.B. (2010) **Fast human brain magnetic resonance responses associated with epileptiform spikes** *Magnet Reson Med* **64**:1728–1738 https://doi.org/10.1002/mrm.22561

27. Toi P.T., Jang H.J., Min K., Kim S.-P., Lee S.-K., Lee J., Kwag J., Park J.-Y. (2022) **In vivo direct imaging of neuronal activity at high temporospatial resolution** *Science* **378**:160–168 https://doi.org/10.1126/science.abh4340

28. Paley M.N.J., Chow L.S., Whitby E.H., Cook G.G. (2009) **Modelling of axonal fields in the optic nerve for direct MR detection studies** *Image and Vision Computing* **27**:331–341 https://doi.org/10.1016/j.imavis.2008.05.001

29. Le Bihan D., Urayama S.-i., Aso T., Hanakawa T., Fukuyama H. (2006) **Direct and fast detection of neuronal activation in the human brain with diffusion MRI** *P Natl Acad Sci USA* **103**:8263–8268 https://doi.org/10.1073/pnas.0600644103

30. Bai R., Stewart C.V., Plenz D., Basser P.J. (2016) **Assessing the sensitivity of diffusion MRI to detect neuronal activity directly** *P Natl Acad Sci USA* **113**:E1728–E1737 https://doi.org/10.1073/pnas.1519890113

31. Chu R., de Zwart J.A., van Gelderen P., Fukunaga M., Kellman P., Holroyd T., Duyn J.H. (2004) **Hunting for neuronal currents: Absence of rapid MRI signal changes during visual-evoked response** *NeuroImage* **23**:1059–1067 https://doi.org/10.1016/j.neuroimage.2004.07.003

32. Konn D., Leach S., Gowland P., Bowtell R. (2004) **Initial attempts at directly detecting alpha wave activity in the brain using MRI** *Magnetic Resonance Imaging* **22**:1413–1427 https://doi.org/10.1016/j.mri.2004.10.012

33. Parkes L.M., de Lange F.P., Fries P., Toni I., Norris D.G. (2007) **Inability to directly detect magnetic field changes associated with neuronal activity** *Magnet Reson Med* **57**:411–416 https://doi.org/10.1002/mrm.21129

34. Miller K.L., Bulte D.P., Devlin H., Robson M.D., Wise R.G., Woolrich M.W., Jezzard P., Behrens T.E.J. (2007) **Evidence for a vascular contribution to diffusion FMRI at high b value** *P Natl Acad Sci USA* **104**:20967–20972 https://doi.org/10.1073/pnas.0707257105

35. Roth B.J., Basser P.J. (2009) **Mechanical model of neural tissue displacement during Lorentz effect imaging** *Magnet Reson Med* **61**:59–64 https://doi.org/10.1002/mrm.21772

36. Luo Q., Lu H., Lu H., Senseman D., Worsley K., Yang Y., Gao J.-H. (2009) **Physiologically evoked neuronal current MRI in a bloodless turtle brain: Detectable or not?** *NeuroImage* **47**:1268–1276 https://doi.org/10.1016/j.neuroimage.2009.06.017

37. Lesage F., Lazdunski M. (2000) **Molecular and functional properties of two-pore-domain potassium channels** *American Journal of Physiology: Renal Physiology* **279**:F793–F801 https://doi.org/10.1152/ajprenal.2000.279.5.F793

38. Ma X.-Y., Yu J.-M., Zhang S.-Z., Liu X.-Y., Wu B.-H., Wei X.-L., Yan J.-Q., Sun H.-L., Yan H.-T., Zheng J.-Q. (2011) **External Ba2+ block of the two-pore domain potassium channel TREK-1 defines conformational transition in its selectivity filter** *Journal of Biological Chemistry* **286**:39813–39822 https://doi.org/10.1074/jbc.M111.264788

39. Vaughan P.F.T., Kaye D.F., Ball S.G., Reeve H.L., Peers C. (1995) **The effect of barium on [3H]noradrenalin release from the human neuroblastoma SH-SY5Y** *European Journal of Neuroscience* **7**:875–880 https://doi.org/10.1111/j.1460-9568.1995.tb01074.x

40. Pottosin I.I., Bonales-Alatorre E., Valencia-Cruz G., Mendoza-Magaña M.L., Dobrovinskaya O.R. (2008) **TRESK-like potassium channels in leukemic T cells** *Pflügers Archiv* **456**:1037–1048 https://doi.org/10.1007/s00424-008-0481-x

41. Bradbury M.W.B., Segal M.B., Wilson J. (1972) **Transport of potassium at the blood-brain barrier** *Journal of Physiology* **221**:617–632 https://doi.org/10.1113/jphysiol1972.sp009771

42. Filippidis A.S., Zarogiannis S.G., Ioannou M., Gourgoulianis K., Molyvdas P.-A., Hatzoglou C. (2012) **Permeability of the arachnoid and pia mater** *The role of ion channels in the leptomeningeal physiology. Child's Nervous System* **28**:533–540 https://doi.org/10.1007/s00381-012-1688-x

43. Walz W. (2000) **Role of astrocytes in the clearance of excess extracellular potassium** *Neurochemistry International* **36**:291–300 https://doi.org/10.1016/S0197-0186(99)00137-0

44. O'Donnell M.E., Alvarez-Leefmans F.J., Delpire E. (2009) **Ion and Water Transport across the Blood-Brain Barrier** *In Physiology and Pathology of Chloride Transporters and Channels in the Nervous System* Academic Press :585–606 https://doi.org/10.1016/B978-0-12-374373-2.00030-3

45. Le Bihan D. (2012) **Diffusion, confusion and functional MRI** *NeuroImage* **62**:1131–1136 https://doi.org/10.1016/j.neuroimage.2011.09.058

46. Mangia S. *et al.* (2012) **Functional MRI with SWIFT** *Proceedings of International Society of Magnetic Resonance in Medicine* **20**

47. Mathur-De Vré R. (1980) **The NMR Studies of water in biological systems** *Progress in Biophysics and Molecular Biology* **35**:103–134 https://doi.org/10.1016/0079-6107(80)90004-8

48. Lang F., Busch G.L., Ritter M., Völkl H., Waldegger S., Gulbins E., Häussinger D. (1998) **Functional significance of cell volume regulatory mechanisms** *Physiological Reviews* **78**:247–306 https://doi.org/10.1152/physrev.1998.78.1.247

49. Fraser J.A., Huang C.L.-H. (2004) **A quantitative analysis of cell volume and resting potential determination and regulation in excitable cells** *Journal of Physiology* **559**:459–478 https://doi.org/10.1113/jphysiol.2004.065706

50. Hoffmann E.K., Lambert I.H., Pedersen S.F. (2009) **Physiology of cell volume regulation in vertebrates** *Physiological Reviews* **89**:193–277 https://doi.org/10.1152/physrev.00037.2007

51. Lee S.-H., Han M.-J., Lee J., Lee S.-K. (2020) **Experimental setup for bulk susceptibility effect-minimized, multi-orientation MRI of ex vivo tissue samples** *Medical Physics* **47**:3032–3043 https://doi.org/10.1002/mp.14174

52. Li K., Zu Z., Xu J., Janve V.A., Gore J.C., Does M.D., Gochberg D.F. (2010) **Optimized inversion recovery sequences for quantitative T1 and magnetization transfer imaging** *Magnetic Resonanace in Medicine* **64**:491–500 https://doi.org/10.1002/mrm.22440

53. Dreier J.P., Körner K., Görner A., Lindauer U., Weih M., Villringer A., Dirnagl U. (1995) **Nitric oxide modulates the CBF response to increased extracellular potassium** *J Cerebr Blood F Met* **15**:914–919 https://doi.org/10.1038/jcbfm.1995.116

54. Redmond L., Kashani A.H., Ghosh A. (2002) **Calcium regulation of dendritic growth via CaM kinase IV and CREB-mediated transcription** *Neuron* **34**:999–1010 https://doi.org/10.1016/s0896-6273(02)00737-7

55. Mostany R., Portera-Cailliau C. (2008) **A craniotomy surgery procedure for chronic brain imaging** *Journal of Visualized Experiments* https://doi.org/10.3791/680

56. Stanisz G.J., Yoon R.S., Joy M.L.G., Henkelman R.M. (2002) **Why does MTR change with neuronal depolarization?** *Magnet Reson Med* **47**:472–475 https://doi.org/10.1002/mrm.10071

57. Autio J.A., Shatillo A., Giniatullin R., Gröhn O.H. (2014) **Parenchymal spin-lock fMRI signals associated with cortical spreading depression** *Journal of Cerebral Blood Flow & Metabolism* **34**:768–775 https://doi.org/10.1038/jcbfm.2014.16

58. McPhee K.C., Wilman A.H. (2017) **Transverse relaxation and flip angle mapping: Evaluation of simultaneous and independent methods using multiple spin echoes** *Magnet Reson Med* **77**:2057–2065 https://doi.org/10.1002/mrm.26285

59. Edzes H.T., Samulski E.T. (1977) **Cross relaxation and spin diffusion in the proton NMR or hydrated collagen** *Nature* **265**:521–523 https://doi.org/10.1038/265521a0

60. Gochberg D.F., Gore J.C. (2003) **Quantitative imaging of magnetization transfer using an inversion recovery sequence** *Magnet Reson Med* **49**:501–505 https://doi.org/10.1002/mrm.10386

61. Hamill O.P., Marty A., Neher E., Sakmann B., Sigworth F.J. (1981) **Improved patch-clamp techniques for high-resolution current recording from cells and cell-free membrane patches** *Pflügers Archiv* **391**:85–100 https://doi.org/10.1007/BF00656997

Editors

Reviewing Editor
Timothy Behrens
University of Oxford, Oxford, United Kingdom

Senior Editor
Tamar Makin
University of Cambridge, Cambridge, United Kingdom

Reviewer #1 (Public review):

Summary:

This paper examines changes in relaxation time (T1 and T2) and magnetization transfer parameters that occur in a model system and in vivo when cells or tissue are depolarized using an equimolar extracellular solution with different concentrations of the depolarizing ion K+. The motivation is to explain T2 changes that have previously been observed by the authors in an in vivo model with neural stimulation (DIANA) and to try provide a mechanism to explain those changes.

Strengths:

The authors argue that the use of various concentrations of KCL in the extracellular fluid depolarize or hyperpolarize the cell pellets used and that this change in membrane potential is the driving force for the T2 (and T1-supplementary material) changes observed. In particular, they report an increase in T2 with increasing KCL concentration in the extracellular fluid (ECF) of pellets of SH-SY5Y cells. To offset the increasing osmolarity of the ECF due to the increase in KCL, the NaCL molarity of the ECF is proportionally reduced. The authors measure the intracellular voltage using patch clamp recordings, which is a gold standard. With 80 mM of KCL in the ECF, a change in T2 of the cell pellets of ~10 ms is

observed with the intracellular potential recorded as about -6 mv. A very large T1 increase of ~90 ms is reported under the same conditions. The PSR (ratio of hydrogen protons on macromolecules to free water) decreases by about 10% at this 80 mM KCL concentration. Similar results are seen in a Jurkat cell line and similar, but far smaller changes are observed in vivo, for a variety of reasons discussed. As a final control, T1 and T2 values are measured in the various equimolar KCL solutions. As expected, no significant changes in T1 and T2 of the ECF were observed for these concentrations.

Weaknesses:

While the concepts presented are interesting, and the actual experimental methods seem to be nicely executed, the conclusions are not supported by the data for a number of reasons. This is not to say that the data isn't consistent with the conclusions, but there are other controls not included that would be necessary to draw the conclusion that it is membrane potential that is driving these T1 and T2 changes. Unfortunately for these authors, similar experiments conducted in 2008 (Stroman et al. Magn. Reson. in Med. 59:700-706) found similar results (increased T2 with KCL) but with a different mechanism, that they provide definite proof for. This study was not referenced in the current work.

It is well established that cells swell/shrink upon depolarization/hyperpolarization. Cell swelling is accompanied by increased light transmittance in vivo, and this should be true in the pellet system as well. In a beautiful series of experiments, Stroman et al. (2008) showed in perfused brain slices that the cells swell upon equimolar KCL depolarization and the light transmittance increases. The time course of these changes is quite slow, of the order of many minutes, both for the T2-weighted MRI signal and for the light transmittance. Stroman et al. also show that hypoosmotic changes produce the exact same timecourse as the KCL depolarization changes (and vice versa for the hyperosmotic changes - which cause cell shrinkage). Their conclusion, therefore, was that cell swelling (not membrane potential) was the cause of the T2-weighted changes observed, and that these were relatively slow (on the scale of many minutes).

What are the implications for the current study? Well, for one, the authors cannot exclude cell swelling as the mechanism for T2 changes, as they have not measured that. It is however well established that cell swelling occurs during depolarization, so this is not in question. Water in the pelletized cells is in slow/intermediate exchange with the ECF, and the solutions for the two compartment relaxation model for this are well established (see Menon and Allen, Magn. Reson. in Med. 20:214-227 (1991). The T2 relaxation times should be multiexponential (see point (3) further below). The current work cannot exclude cell swelling as the mechanism for T2 changes (it is mentioned in the paper, but not dealt with). Water entering cells dilutes the protein structures, changes rotational correlation times of the proteins in the cell and is known to increase T2. The PSR confirms that this is indeed happening, so the data in this work is completely consistent with the Stroman work and completely consistent with cell swelling associated with depolarization. The authors should have performed light scattering studies to demonstrate the presence or absence of cell swelling. Measuring intracellular potential is not enough to clarify the mechanism.

So why does it matter whether the mechanism is cell swelling or membrane potential? The reason is response time. Cell swelling due to depolarization is a slow process, slower than hemodynamic responses that characterize BOLD. In fact, cell swelling under normal homeostatic conditions in vivo is virtually non-existent. Only sustained depolarization events typically associated with non-naturalistic stimuli or brain dysfunction produce cell swelling. Membrane potential changes associated with neural activity, on the other hand, are very fast. In this manuscript, the authors have convincingly shown a signal change that is virtually the same as what was seen in the Stroman publication, but they have not shown that there is a response that can be detected with anything approaching the timescale of an action potential.

So one cannot definitely say that the changes observed are due to membrane potential. One can only say they are consistent with cell swelling, regardless of what causes the cell swelling.

For this mechanism to be relevant to explaining DIANA, one needs to show that the cell swelling changes occur within a millisecond, which has never been reported. If one knows the populations of ECF and pellet, the T2s of the ECF and pellet and the volume change of the cells in the pellet, one can model any expected T2 changes due to neuronal activity. I think one would find that these are minuscule within the context of an action potential, or even bulk action potential.

There are a few smaller issues that should be addressed.
(1) Why were complicated imaging sequences used to measure T1 and T2? On a Bruker system it should be possible to do very simple acquisitions with hard pulses (which will not need dictionaries and such to get quantitative numbers). Of course, this can only be done sample by sample and would take longer, but it avoids a lot of complication to correct the RF pulses used for imaging, which leads me to the 2nd point.
(2) Figure S1 (H) is unlike any exponential T2 decay I have seen in almost 40 years of making T2 measurements. The strange plateau at the beginning and the bump around TE = 25 ms are odd. These could just be noise, but the fitted curve exactly reproduces these features. A monoexponential T2 decay cannot, by definition, produce a fit shaped like this.
(3) As noted earlier, layered samples produce biexponential T2 decays and monoexponential T1 decays. I don't quite see how this was accounted for in the fitting of the data from the pellet preparations. I realize that these are spatially resolved measurements, but the imaging slice shown seems to be at the boundary of the pellet and the extracellular media and there definitely should be a biexponential water proton decay curve. Only 5 echo times were used, so this is part of the problem, but it does mean that the T2 reported is a population fraction weighted average of the T2 in the two compartments.
(4) Delta T1 and T2 values are presented for the pellets in wells, but no absolute values are presented for either the pellets or the KCL solutions that I could find.

https://doi.org/10.7554/eLife.101642.1.sa2

Reviewer #2 (Public review):

Summary:

Min et al. attempt to demonstrate that magnetic resonance imaging (MRI) can detect changes in neuronal membrane potentials. They approach this goal by studying how MRI contrast and cellular potentials together respond to treatment of cultured cells with ionic solutions. The authors specifically study two MRI-based measurements: (A) the transverse (T2) relaxation rate, which reflects microscopic magnetic fields caused by solutes and biological structures; and (B) the fraction or "pool size ratio" (PSR) of water molecules estimated to be bound to macromolecules, using an MRI technique called magnetization transfer (MT) imaging. They see that depolarizing K+ and Ba2+ concentrations lead to T2 increases and PSR decreases that vary approximately linearly with voltage in a neuroblastoma cell line and that change similarly in a second cell type. They also show that depolarizing potassium concentrations evoke reversible T2 increases in rat brains and that these changes are reversed when potassium is renormalized. Min et al. argue that this implies that membrane potential changes cause the MRI effects, providing a potential basis for detecting cellular voltages by noninvasive imaging. If this were true, it would help validate a recent paper published by some of the authors (Toi et al., Science 378:160-8, 2022), in which they claimed to be able to detect millisecond-scale neuronal responses by MRI.

Strengths:

The discovery of a mechanism for relating cellular membrane potential to MRI contrast could yield an important means for studying functions of the nervous system. Achieving this has been a longstanding goal in the MRI community, but previous strategies have proven too weak or insufficiently reproducible for neuroscientific or clinical applications. The current paper suggests remarkably that one of the simplest and most widely used MRI contrast mechanisms-T2 weighted imaging-may indicate membrane potentials if measured in the absence of the hemodynamic signals that most functional MRI (fMRI) experiments rely on. The authors make their case using a diverse set of quantitative tests that include controls for ion and cell type-specificity of their in vitro results and reversibility of MRI changes observed in vivo.

Weaknesses:

The major weakness of the paper is that it uses correlational data to conclude that there is a causational relationship between membrane potential and MRI contrast. Alternative explanations that could explain the authors' findings are not adequately considered. Most notably, depolarizing ionic solutions can also induce changes in cellular volume and tissue structure that in turn alter MRI contrast properties similarly to the results shown here. For example, a study by Stroman et al. (Magn Reson Med 59:700-6, 2008) reported reversible potassium-dependent T2 increases in neural tissue that correlate closely with light scattering-based indications of cell swelling. Phi Van et al. (Sci Adv 10:eadl2034, 2024) showed that potassium addition to one of the cell lines used here likewise leads to cell size increases and T2 increases. Such effects could in principle account for Min et al.'s results, and indeed it is difficult to see how they would not contribute, but they occur on a time scale far too slow to yield useful indications of membrane potential. The authors' observation that PSR correlates negatively with T2 in their experiments is also consistent with this explanation, given the inverse relationship usually observed (and mechanistically expected) between these two parameters. If the authors could show a tight correspondence between millisecond-scale membrane potential changes and MRI contrast, their argument for a causal connection or a useful correlational relationship between membrane potential and image contrast would be much stronger. As it is, however, the article does not succeed in demonstrating that membrane potential changes can be detected by MRI.

https://doi.org/10.7554/eLife.101642.1.sa1

Author response:

> ***Public Reviews:***
>
> ***Reviewer #1 (Public review):***
>
> *Summary:*
>
> *This paper examines changes in relaxation time (T1 and T2) and magnetization transfer parameters that occur in a model system and in vivo when cells or tissue are depolarized using an equimolar extracellular solution with different concentrations of the depolarizing ion K+. The motivation is to explain T2 changes that have previously been observed by the authors in an in vivo model with neural stimulation (DIANA) and to try provide a mechanism to explain those changes.*
>
> *Strengths:*
>
> *The authors argue that the use of various concentrations of KCL in the extracellular fluid depolarize or hyperpolarize the cell pellets used and that this change in membrane potential is the driving force for the T2 (and T1-supplementary material) changes*

observed. In particular, they report an increase in T2 with increasing KCL concentration in the extracellular fluid (ECF) of pellets of SH-SY5Y cells. To offset the increasing osmolarity of the ECF due to the increase in KCL, the NaCL molarity of the ECF is proportionally reduced. The authors measure the intracellular voltage using patch clamp recordings, which is a gold standard. With 80 mM of KCL in the ECF, a change in T2 of the cell pellets of ~10 ms is observed with the intracellular potential recorded as about -6 mv. A very large T1 increase of ~90 ms is reported under the same conditions. The PSR (ratio of hydrogen protons on macromolecules to free water) decreases by about 10% at this 80 mM KCL concentration. Similar results are seen in a Jurkat cell line and similar, but far smaller changes are observed in vivo, for a variety of reasons discussed. As a final control, T1 and T2 values are measured in the various equimolar KCL solutions. As expected, no significant changes in T1 and T2 of the ECF were observed for these concentrations.

Weaknesses:

While the concepts presented are interesting, and the actual experimental methods seem to be nicely executed, the conclusions are not supported by the data for a number of reasons. This is not to say that the data isn't consistent with the conclusions, but there are other controls not included that would be necessary to draw the conclusion that it is membrane potential that is driving these T1 and T2 changes. Unfortunately for these authors, similar experiments conducted in 2008 (Stroman et al. Magn. Reson. in Med. 59:700-706) found similar results (increased T2 with KCL) but with a different mechanism, that they provide definite proof for. This study was not referenced in the current work.

It is well established that cells swell/shrink upon depolarization/hyperpolarization. Cell swelling is accompanied by increased light transmittance in vivo, and this should be true in the pellet system as well. In a beautiful series of experiments, Stroman et al. (2008) showed in perfused brain slices that the cells swell upon equimolar KCL depolarization and the light transmittance increases. The time course of these changes is quite slow, of the order of many minutes, both for the T2-weighted MRI signal and for the light transmittance. Stroman et al. also show that hypoosmotic changes produce the exact same timecourse as the KCL depolarization changes (and vice versa for the hyperosmotic changes - which cause cell shrinkage). Their conclusion, therefore, was that cell swelling (not membrane potential) was the cause of the T2-weighted changes observed, and that these were relatively slow (on the scale of many minutes).

What are the implications for the current study? Well, for one, the authors cannot exclude cell swelling as the mechanism for T2 changes, as they have not measured that. It is however well established that cell swelling occurs during depolarization, so this is not in question. Water in the pelletized cells is in slow/intermediate exchange with the ECF, and the solutions for the two compartment relaxation model for this are well established (see Menon and Allen, Magn. Reson. in Med. 20:214-227 (1991). The T2 relaxation times should be multiexponential (see point (3) further below). The current work cannot exclude cell swelling as the mechanism for T2 changes (it is mentioned in the paper, but not dealt with). Water entering cells dilutes the protein structures, changes rotational correlation times of the proteins in the cell and is known to increase T2. The PSR confirms that this is indeed happening, so the data in this work is completely consistent with the Stroman work and completely consistent with cell swelling associated with depolarization. The authors should have performed light scattering studies to demonstrate the presence or absence of cell swelling. Measuring intracellular potential is not enough to clarify the mechanism.

We appreciate the reviewer's comments. We agree that changes in cell volume due to depolarization and hyperpolarization significantly contribute to the observed changes in T2,

PSR, and T1, especially in pelletized cells. For this reason, we already noted in the Discussion section of the original manuscript that cell volume changes influence the observed MR parameter changes, though this study did not present the magnitude of the cell volume changes. In this regard, we thank the reviewer for introducing the work by Stroman et al. (Magn Reson Med 59:700-706, 2008). When discussing the contribution of the cell volume changes to the observed MR parameter changes, we will additionally discuss the work of Stroman et al. in the revised manuscript.

In addition, we acknowledge that the title and main conclusion of the original manuscript may be misleading, as we did not separately consider the effect of cell volume changes on MR parameters. To more accurately reflect the scope and results of this study and to consider the reviewer 2's suggestion, we will adjust the title to "Responses to membrane potential-modulating ionic solutions measured by magnetic resonance imaging of cultured cells and in vivo rat cortex" and will also revise the relevant phrases in the main text.

Finally, when [K+]-induced membrane potential changes are involved, there seems to be factors other than cell volume changes also appear to influence T2 changes. Our ongoing study shows that there are differences in T2 changes (for the same volume changes) between two different situations: pure osmotic volume changes vs. [K+]-induced volume changes (e.g., hypoosmotic vs. depolarization). Furthermore, this study suggests that mechanisms such as changes in free (primarily intracellular) and bound water within a voxel play an important role in generating this T2 difference. Our group is preparing a manuscript for this follow-up study and will report on it shortly.

> *So why does it matter whether the mechanism is cell swelling or membrane potential? The reason is response time. Cell swelling due to depolarization is a slow process, slower than hemodynamic responses that characterize BOLD. In fact, cell swelling under normal homeostatic conditions in vivo is virtually non-existent. Only sustained depolarization events typically associated with non-naturalistic stimuli or brain dysfunction produce cell swelling. Membrane potential changes associated with neural activity, on the other hand, are very fast. In this manuscript, the authors have convincingly shown a signal change that is virtually the same as what was seen in the Stroman publication, but they have not shown that there is a response that can be detected with anything approaching the timescale of an action potential. So one cannot definitely say that the changes observed are due to membrane potential. One can only say they are consistent with cell swelling, regardless of what causes the cell swelling.*
>
> *For this mechanism to be relevant to explaining DIANA, one needs to show that the cell swelling changes occur within a millisecond, which has never been reported. If one knows the populations of ECF and pellet, the T2s of the ECF and pellet and the volume change of the cells in the pellet, one can model any expected T2 changes due to neuronal activity. I think one would find that these are minuscule within the context of an action potential, or even bulk action potential.*

In the context of cell swelling occurring at rapid response times, if we define cell swelling simply as an "increase in cell volume," there are several studies reporting transient structural (or volumetric) changes (e.g., ~nm diameter change over ~ms duration) in neuron cells during action potential propagation (Akkin et al., Biophys J 93:1347-1353, 2007; Kim et al., Biophys J 92:3122-3129, 2007; Lee et al., IEEE Trans Biomed Eng 58:3000-3003, 2011; Wnek et al., J Polym Sci Part B: Polym Phys 54:7-14, 2015; Yang et al., ACS Nano 12:4186-4193, 2018). These studies show a good correlation between membrane potential changes and cell volume changes (even if very small) at the cellular level within milliseconds.

As mentioned in the Response 1 above, this study does not address rapid dynamic membrane potential changes on the millisecond scale, which we explicitly discussed as one of the

limitations in the Discussion section of the original manuscript. For this reason, we do not claim in this study that we provide the reader with definitive answers about the mechanisms involved in DIANA. Rather, as a first step toward addressing the mechanism of DIANA, this study confirms that there is a good correlation between changes in membrane potential and measurable MR parameters (e.g., T2 and PSR) when using ionic solutions that modulate membrane potential. Identifying T2 changes that occur during millisecond-scale membrane potential changes due to rapid neural activation will be further addressed in future studies.

> *There are a few smaller issues that should be addressed.*
>
> *(1) Why were complicated imaging sequences used to measure T1 and T2? On a Bruker system it should be possible to do very simple acquisitions with hard pulses (which will not need dictionaries and such to get quantitative numbers). Of course, this can only be done sample by sample and would take longer, but it avoids a lot of complication to correct the RF pulses used for imaging, which leads me to the 2nd point.*

We appreciate the reviewer's suggestion regarding imaging sequences. We would like to clarify that dictionaries were used for fitting in vivo T2 decay data, not in vitro data. Sample-by-sample nonlocalized acquisition with hard pulses may be applicable for in vitro measurements. However, for in vivo measurements, a slice-selective multi-echo spin-echo sequence was necessary to acquire T2 maps within a reasonable scan time. Our choice of imaging sequence was guided by the need to spatially resolve MR signals from specific regions of interests while balancing scan time constraints.

> *(2) Figure S1 (H) is unlike any exponential T2 decay I have seen in almost 40 years of making T2 measurements. The strange plateau at the beginning and the bump around TE = 25 ms are odd. These could just be noise, but the fitted curve exactly reproduces these features. A monoexponential T2 decay cannot, by definition, produce a fit shaped like this.*

The T2 decay curves in Figure S1(H) indeed display features that deviate from a simple monoexponential decay. In our in vivo experiments, we used a multi-echo spin-echo sequence with slice-selective excitation and refocusing pulses. In such sequences, the echo train is influenced by stimulated echoes and imperfect slice profiles. This phenomenon is inherent to the pulse sequence rather than being artifacts or fitting errors (Hennig, Concepts Magn Reson 3:125-143, 1991; Lebel and Wilman, Magn Reson Med 64:1005-1014, 2010; McPhee and Wilman, Magn Reson Med 77:2057-2065, 2017). Therefore, we fitted the T2 decay curve using the technique developed by McPhee and Wilman (2017).

> *(3) As noted earlier, layered samples produce biexponential T2 decays and monoexponential T1 decays. I don't quite see how this was accounted for in the fitting of the data from the pellet preparations. I realize that these are spatially resolved measurements, but the imaging slice shown seems to be at the boundary of the pellet and the extracellular media and there definitely should be a biexponential water proton decay curve. Only 5 echo times were used, so this is part of the problem, but it does mean that the T2 reported is a population fraction weighted average of the T2 in the two compartments.*

We understand the reviewer's concern regarding potential biexponential decay due to the presence of different compartments. In our experiments, we carefully positioned the imaging slice sufficiently remote from the pellet-media interface. This approach ensures that the signal predominantly arises from the cells (and interstitial fluid), excluding the influence of extracellular media above the cell pellet. We will clearly describe the imaging slice in the revised manuscript. As mentioned in our Methods section, for in vitro experiments, we

repeated a single-echo spin-echo sequence with 50 difference echo times. While Figure 1C illustrates data from five echo times for visual clarity, the full dataset with all 50 echo times was used for fitting. We will clarify this point in the revised manuscript to avoid any misunderstanding.

> *(4) Delta T1 and T2 values are presented for the pellets in wells, but no absolute values are presented for either the pellets or the KCL solutions that I could find.*

As requested by the reviewer, we will include the absolute values in the revised manuscript.

> ***Reviewer #2 (Public review):***
>
> *Summary:*
>
> *Min et al. attempt to demonstrate that magnetic resonance imaging (MRI) can detect changes in neuronal membrane potentials. They approach this goal by studying how MRI contrast and cellular potentials together respond to treatment of cultured cells with ionic solutions. The authors specifically study two MRI-based measurements: (A) the transverse (T2) relaxation rate, which reflects microscopic magnetic fields caused by solutes and biological structures; and (B) the fraction or "pool size ratio" (PSR) of water molecules estimated to be bound to macromolecules, using an MRI technique called magnetization transfer (MT) imaging. They see that depolarizing K+ and Ba2+ concentrations lead to T2 increases and PSR decreases that vary approximately linearly with voltage in a neuroblastoma cell line and that change similarly in a second cell type. They also show that depolarizing potassium concentrations evoke reversible T2 increases in rat brains and that these changes are reversed when potassium is renormalized. Min et al. argue that this implies that membrane potential changes cause the MRI effects, providing a potential basis for detecting cellular voltages by noninvasive imaging. If this were true, it would help validate a recent paper published by some of the authors (Toi et al., Science 378:160-8, 2022), in which they claimed to be able to detect millisecond-scale neuronal responses by MRI.*
>
> *Strengths:*
>
> *The discovery of a mechanism for relating cellular membrane potential to MRI contrast could yield an important means for studying functions of the nervous system. Achieving this has been a longstanding goal in the MRI community, but previous strategies have proven too weak or insufficiently reproducible for neuroscientific or clinical applications. The current paper suggests remarkably that one of the simplest and most widely used MRI contrast mechanisms-T2 weighted imaging-may indicate membrane potentials if measured in the absence of the hemodynamic signals that most functional MRI (fMRI) experiments rely on. The authors make their case using a diverse set of quantitative tests that include controls for ion and cell type-specificity of their in vitro results and reversibility of MRI changes observed in vivo.*
>
> *Weaknesses:*
>
> *The major weakness of the paper is that it uses correlational data to conclude that there is a causational relationship between membrane potential and MRI contrast. Alternative explanations that could explain the authors' findings are not adequately considered. Most notably, depolarizing ionic solutions can also induce changes in cellular volume and tissue structure that in turn alter MRI contrast properties similarly to the results shown here. For example, a study by Stroman et al. (Magn Reson Med 59:700-6, 2008) reported reversible potassium-dependent T2 increases in neural tissue that correlate closely with light scattering-based indications of cell swelling. Phi Van et al. (Sci Adv 10:eadl2034, 2024) showed that potassium addition to one of the cell lines used here*

> *likewise leads to cell size increases and T2 increases. Such effects could in principle account for Min et al.'s results, and indeed it is difficult to see how they would not contribute, but they occur on a time scale far too slow to yield useful indications of membrane potential. The authors' observation that PSR correlates negatively with T2 in their experiments is also consistent with this explanation, given the inverse relationship usually observed (and mechanistically expected) between these two parameters. If the authors could show a tight correspondence between millisecond-scale membrane potential changes and MRI contrast, their argument for a causal connection or a useful correlational relationship between membrane potential and image contrast would be much stronger. As it is, however, the article does not succeed in demonstrating that membrane potential changes can be detected by MRI.*

We appreciate the reviewer's comments. We agree that changes in cell volume due to depolarization and hyperpolarization significantly contribute to the observed MR parameter changes. For this reason, we have already noted in the Discussion section of the original manuscript that cell volume changes influence the observed MR parameter changes. In this regard, we thank the reviewer for introducing the work by Stroman et al. (Magn Reson Med 59:700-706, 2008) and Phi Van et al. (Sci Adv 10:eadl2034, 2024). When discussing the contribution of the cell volume changes to the observed MR parameter changes, we will additionally discuss both work of Stroman et al. and Phi Van et al. in the revised manuscript.

In addition, this study does not address rapid dynamic membrane potential changes on the millisecond scale, which we explicitly discussed as one of the limitations of this study in the Discussion section of the original manuscript. For this reason, we do not claim in this study that we provide the reader with definitive answers about the mechanisms involved in DIANA. Rather, as a first step toward addressing the mechanism of DIANA, this study confirms that there is a good correlation between changes in membrane potential and measurable MR parameters (although on a slow time scale) when using ionic solutions that modulate membrane potential. Identifying T2 changes that occur during millisecond-scale membrane potential changes due to rapid neural activation will be further addressed in future studies.

Together, we acknowledge that the title and main conclusion of the original manuscript may be misleading. To more accurately reflect the scope and results of this study and to consider the reviewer's suggestion, we will adjust the title to "Responses to membrane potential-modulating ionic solutions measured by magnetic resonance imaging of cultured cells and in vivo rat cortex" and will also revise the relevant phrases in the main text.

https://doi.org/10.7554/eLife.101642.1.sa0